Morin-Loaded Chitosan-Poloxamer Hydrogel as an Osteoinductive Delivery System for Endodontic Applications

Short running title: Morin-loaded hydrogels for endodontics

Jesse Augusto Pereira[1], Victor Martin[2,3*], Rita Araújo[2,3], Liliana Grenho[2,3], Pedro Gomes[2,3], Joana Marto[4], Maria Helena Fernandes[2,3], Catarina Santos[5,6], Cristiane Duque[1,7*].

[1]Department of Preventive and Restorative Dentistry, Araçatuba Dental School, São Paulo State University (UNESP), Araçatuba, São Paulo, Brazil. (jesseaugusto.p@gmail.com, JAP; cduque@ucp.pt, CD)

[2]BoneLab, Faculdade de Medicina Dentária, Universidade do Porto, 4200-393 Porto, Portugal, rita_araujosilva@sapo.pt, RA; lgrenho@fmd.up.pt, LG; pgomes@fmd.up.pt, PG; mhfernandes@fmd.up.pt, MHF)

[3]LAQV/REQUIMTE, Faculdade de Medicina Dentária, Universidade do Porto, Rua Dr. Manuel Pereira da Silva, 4200-393 Porto, Portugal.

[4]Research Institute for Medicines (iMed.ULisboa), Faculty of Pharmacy, Universidade de Lisboa, 1649-003 Lisbon, Portugal. (jmmarto@ff.ulisboa.pt, JM)

[5]EST Setúbal, CDP2T, Instituto Politécnico de Setúbal, 2910-761 Setúbal, Portugal. (catarina.santos@estsetubal.ips.pt, CS)

[6]CQE Instituto Superior Técnico, Universidade de Lisboa, 1049-001 Lisboa, Portugal.

[7]Faculty of Dental Medicine, Center for Interdisciplinary Research in Health (CIIS), Universidade Católica Portuguesa, Viseu, Portugal.

***Corresponding authors:**

Cristiane Duque

Faculty of Dental Medicine, Centre for Interdisciplinary Research in Health (CIIS), Universidade Católica Portuguesa (Catholic University of Portugal).

Rua da Circunvalação, s/n, 3504-505, Viseu, Portugal.

Tel: (+351) 232 419 500.

E-mail: cristianeduque@yahoo.com.br, cduque@ucp.pt, cristiane.duque@unesp.br

Orcid iD: 0000-0002-2575-279X
Victor Martin
BoneLab, Faculdade de Medicina Dentária, Universidade do Porto.
Address: Rua Dr. Manuel Pereira da Silva, 4200-393 Porto, Portugal.
Tel: (+351) 220 901 100.
E-mail: vmartin@fmd.up.pt
Orcid iD: 0000-0001-6910-1705

Funding

This work received financial support from FCT/MCTES (UIDB/50006/2020 DOI 10.54499/UIDB/50006/2020) through national funds.

Acknowledgements

The authors acknowledge the support of the i3S Scientific Platform HEMS - Histology and Electron Microscopy Department.

This work received support and help from FCT/MCTES (LA/P/0008/2020 DOI 10.54499/LA/P/0008/2020 and UIDP/50006/2020 DOI 10.54499/UIDP/50006/2020), through national funds.

Data Availability Statement

The data presented in this study are available on request from the corresponding authors.

Conflicts of Interest

The authors declare that they have no conflict of interest or financial interests to disclose.

Abstract

Objectives: Considering the search for new biocompatible intracanal medicaments that can preserve remaining cells and stimulate bone tissue repair in the periapical region, this study aimed to synthesize and characterize the physicochemical properties of morin-loaded chitosan-poloxamer hydrogel (MCP) as well as to evaluate its osteogenic potential.

Methods: Morin hydrate (M) was loaded into chitosan-poloxamer (CP) hydrogel and the resulting particles were characterized by infrared spectroscopy (FTIR), UV−vis spectrophotometer and scanning electron microscopy. Biological assays evaluated the metabolic activity, cell morphology and alkaline phosphatase (ALP) activity of human bone marrow stem cells (HBMSC) in three different settings, such as the exposure to dissolved morin, hydrogel's leachates and assembled particles by indirect contact. Cells cultured in standard culture conditions were used as control. The effect of CP and MCP particles on the formation of collagenous and mineralized tissues was also assessed within the organotypic model of segmented embryonic chick femora. Datasets were assessed for one-way analysis of variance (ANOVA), followed by Tukey's post hoc test ($p<0.05$).

Results: Morin at 50 µg/mL was cytocompatible and increased ALP activity. CP and MCP particles showed stability, and morin was entrapped in the hydrogel matrix without changing its chemical structure. Cultures treated with 30-min CP and MCP hydrogel leachates presented significantly higher metabolic activity compared to control. By indirect contact, CP particles increased metabolic activity, but only MCP particles induced an upregulation of ALP activity in comparison to control. The amount of collagenous tissue and mineralized area on the fractured embryonic chick femora was greater in MCP particles compared to CP counterparts.

Significance: Chitosan-poloxamer platforms are suitable systems to delivery morin, enhancing cell proliferation and bone mineralization, which upholds its application as intracanal medication for endodontic purposes.

Keywords: Morin; Chitosan; Poloxamer; Biocompatibility; Osteogenesis; Stem cells; Drug-delivery.

Highlights

- The MCP hydrogel exhibited osteoblastic cytocompatibility to human bone marrow stem cells.
- The MCP hydrogel induced bone formation within the embryonic chick femora organotypic model.
- The MCP hydrogel holds potential as a medication for endodontic purposes.

1. Introduction

Apical periodontitis is a chronic inflammatory process that develops around the dental apex, commonly in permanent teeth, mainly triggered by bacterial invasion from the pulp affected by caries or trauma [1]. In addition to the direct harmful effect of bacterial products, the active immune inflammatory response in the region generates an intracellular signaling cascade, involving the production of inflammatory cytokines that are related to the migration of inflammatory cells and osteoclastogenesis [2,3]. This process culminates in the disruption of bone homeostasis and the upregulation of resorption factors with consequent bone loss and the formation of periapical lesions [4].

The treatment of teeth with apical periodontitis involves the chemical-mechanical preparation of the root canals with bactericidal irrigating solutions and subsequent application of intracanal medication. In immature permanent teeth with apical periodontitis, clinical treatment is more challenging, since these teeth have short roots with thin, parallel dentin walls that make irrigation procedures difficult, and the presence of an open and still developing apex. Traditional endodontic treatment (apexification) uses irrigating chemical substances such as sodium hypochlorite or chlorhexidine. However, when used at the recommended high concentrations, these substances can compromise the viability of the remaining cells in the pulp tissue or adjacent areas, potentially disrupting root formation [5, 6]. Traditionally, periodic exchanges of calcium hydroxide with intracanal medication are also recommended due to its physicochemical and antimicrobial properties. However, its alkalinity also hampers the viability of residual cells and does not promote continued root development [7]. Therefore, the development of alternative biocompatible solutions and intracanal

medicaments is highly relevant, as they can preserve remaining cells to guide root formation and stimulate tissue repair in the periapical region [8,9].

Plant-derived bioactive compounds, such as flavonoids, have received attention in the literature due to their wide range of therapeutic applications. Studies have highlighted several pharmacological properties of flavonoids - polyphenols present in fruits, seeds, and vegetables - such as antimicrobial, antioxidant, anti-inflammatory, osteogenic and antiosteoclastogenic actions, among others [10-12]. Flavonoids include flavones, flavonols, flavanones, flavanonol, flavanols, anthocyanidins and chalcones [12]. Morin is a flavonol (3,5,7,2',4'-pentahydroxyflavone) found in several plants, including *Morus alba L* (white mulberry), *Prunus dulcis* (almond), *Castanea sativa* (sweet chestnut), *Psidium guajava* (guava), among others [13, 14]. Morin has demonstrated radical scavenging, antioxidant, anti-inflammatory, anti-cancerous, antimicrobial, antidiabetic, anti-arthritis, cardioprotective, neuroprotective, nephroprotective, and hepatoprotective effects [14, 15]. Furthermore, its applicability as a medicine also becomes viable due to its low cytotoxicity [16,17].

Morin was also employed as a medication for dentistry applications. Studies have demonstrated the inhibitory effect of morin on planktonic bacteria commonly isolated from oral infections [10,18-20] and on dental biofilm formation [21-24]. Moreover, the ability of morin in repairing bone defects was demonstrated in mice by inducing differentiation of mesenchymal cells and by activating classical signaling pathways, which culminated in the upregulation of genes related to bone mineralization, as well as in the decrease of bone resorption markers [11, 25].

To take advantage of the full potential of morin, therapeutic applications must focus on local delivery approaches, relying on biocompatible and biodegradable delivery carriers, such as hydrogels. These systems can improve the solubility and stability of phytochemicals, in addition to protecting them from early degradation by body fluids [25]. One of the most studied natural polymers is chitosan, a polysaccharide of animal origin obtained from the chitin of the exoskeleton of crustaceans [25,26]. Chitosan has the ability to form a hydrogel under suitable conditions, however it has low mechanical strength and poor absorption in water solutions [26]. Poloxamer 407 is another polymer commonly used in various drug delivery systems, including in combination with chitosan. It offers innumerous advantages, such as thermoreversibility, low toxicity,

biocompatibility, ability to enhance biomolecules solubilization and the ability to prolong the release profile for many applications [27,28]. Thus, the present study aimed to develop and characterize an innovative hydrogel loaded with morin, with osteogenic effects, devised to be an alternative treatment for apical periodontitis. The carrier consists of a mixture of a natural polymer, chitosan, and a synthetic polymer, poloxamer 407, to provide low toxicity, biocompatibility, and an optimal profile for the controlled release of morin.

2. Methods

2.1. Morin and controls

Unless otherwise specified, compounds and reagents were purchased from Sigma-Aldrich® (St. Louis, MO, USA) and cell culture media from ThermoFisher Scientific® (Waltham, MA, USA). Morin hydrate powder (#M4008) was dissolved in dimethyl sulfoxide (DMSO) cell culture-grade to obtain a stock solution of 25.2 mg/mL. Then, the stock solution was sterilized using a 0.2 µm syringe filter. Working solutions at selected concentrations were obtained by diluting the stock solution with α-Minimal Essential Medium (α-MEM) culture medium for cytological assays. The percentage of DMSO in working solutions was kept < 0.05% v/v. Control cultures receiving analogous volume of DMSO without added morin were considered as control groups (set as 100% growth/metabolism). The assays were performed in three independent days.

2.2. Synthesis of Morin-loaded chitosan-poloxamer (MCP) hydrogels and assembly of MCP particles

Morin-loaded chitosan-poloxamer hydrogels were synthesized via an ionotropic gelation technique [29]. First, chitosan from shrimp exoskeleton (molecular weight 10-50kd, viscosity 20-300cps, deacetylation degree 80-95%) (1% wt./vol) was dissolved in a solution of acetic acid (1% wt./vol) using a mechanical stirrer (600 rpm) for about 3 h. Parallelly, poloxamer 407 (HP-407, Kolliphor 407: contains nominally 95 to 105 ethylene oxide units and 54 to 60 propylene oxide units, with a rough concentration of oxyethylene of 71.5 to 74.9 %) (10% wt./vol) was mixed with morin (2 mg/mL) under magnetic stirring (600 rpm) at room temperature. Afterwards, chitosan solution was

combined with the morin-poloxamer 407 solution in a 1:1 (vol/vol) ratio and stirred for 5 min to yield a morin-chitosan-poloxamer (MCP) hydrogel.

The MCP hydrogel (prepared as described above) was formulated as particles for transportation and physicochemical analysis by dripping it into a 1 M NaOH solution. The resulting MCP particles were subjected to magnetic stirring for 10 minutes at 600 rpm in the NaOH solution. The supernatant was then discarded, and the MCP particles were washed with Milli-Q water. The washing procedure was repeated three times. Finally, particles were dried in a desiccator overnight. In the present work, the gel particles were prepared with aliquots of 50 µL of the respective solution. The same procedure was applied to produce chitosan-poloxamer (CP) hydrogel, as well as the designated CP particles, without morin.

2.3. Physicochemical characterization of MCP hydrogels and particles

Fourier transformed infrared spectroscopy (FTIR) spectra of morin, CP and MCP hydrogels were recorded on a Nicolet (Thermo-Electron Corp, ThermoFisher) spectrometer using with an attenuated total reflectance (ATR) apparatus. The spectra were collected in the scanning range 4000 cm^{-1} to 600 cm^{-1}, with a resolution of 4 cm^{-1} and 128 scans. The surface of CP and MCP particles was observed using a scanning electron microscope (SEM). The EDS analysis of morin was carried out using the same equipment. The CP and MCP particles were coated with a thin conductive chromium or gold/palladium film (Model E5100 Sputter Coater, Polaron, Quorum Technologies) and scanned under a Phenom ProX G6 Desktop electron microscope operating at a voltage 20 kV. The surface charge of CP and MCP particles was evaluated through zeta potential measurements using a Malvern ZetaSizer Nano ZS instrument. Measurements were carried out at 25 °C, in triplicate. Moreover, the morin content encapsulated within the MCP particles was assessed using a UV−vis spectrophotometer (GENESYS™ 50 UV-Visible, ThermoFisher). In this assay, MCP particles were incubated in 1 mL of PBS and centrifuged at 3,000 rpm, forcing the complete release of the loaded morin. The absorbance of the supernatant was measured at 410 nm (the peak absorption of morin in PBS). Subsequently, the encapsulation efficiency was calculated using the formula provided below:

$((W-w_s)/W)X\ 100$

where W is the amount of the morin initially added to chitosan-poloxamer (MCP) and w_s is the amount of the morin present in the supernatant of the MCP particles.

2.4. Release profile of morin from the MCP particles

To quantify the morin release, MCP and CP particles were prepared as described in the section 2.2. Each unit of the particles was incubated with 1 mL of PBS at 37 ºC. Aliquots of 100 µL of the supernatant were collected at predetermined intervals (30 min, 1 h, 3 h, 6 h, 24 h), and the withdrawn volume was replaced with fresh PBS. Morin content in the collected leachates was determined by measuring the supernatant's absorbance at 410 nm using a microplate reader (Synergy HT, BioTek). A calibration curve (R^2=0.999) was prepared upon a concentration range of 0.97–250 µg/mL of morin for the conversion of the absorbance values into morin concentrations. Results are presented as the cumulative release (%) of morin. Assays were performed in triplicate.

2.5. In vitro assessment using HBMSCs cultures

Human bone marrow stem cells (HBMSCs, Lonza, PT-2501) from the 5th passage were used in the cellular experiments. HBMSCs were expanded in α-MEM supplemented with 10% (vol/vol) fetal bovine serum (FBS), penicillin (100 IU/mL), streptomycin, (100 µg/mL), and amphotericin B (2.5 µg/mL). Cells were kept at 37 °C with 5% CO_2 in air. Once the cultures reached 70% confluence, cells were trypsinized and sub-cultured at a density of 10,000 cells/cm^2, and the culture medium was further supplemented with osteogenic inducers (10 mM β-glycerophosphate, 50 µg/mL of ascorbic acid and 10 nM dexamethasone). Three distinct experimental approaches were set: assays comprising exposure to 1) morin at 10, 50 and 100 µg/mL[1] dissolved in culture media; 2) hydrogel's leachates, collected after incubating 50 µL of each CP and MCP hydrogel in 1 mL of culture medium at 37 ºC for 30, 60, 180, and 360 minutes; and 3) assembled particles (CP and MCP) evaluated through indirect contact, in which cells were grown at the bottom of 24-well plates attached with permeable inserts (Transwell 6.5 mm insert, 0.4 µm permeable membrane, Costar), where the particles were placed [30].

2.5.1. *Metabolic activity*

The metabolic activity of HBMSCs cultures was assessed using the resazurin assay. At selected timepoints, culture media were replaced by fresh media containing 10% v/v of 100 µg/mL resazurin solution (Sigma-Aldrich). Cells were incubated for 3 h at 37 °C. Then, media were collected, and their fluorescence was measured at 530/590 nm (excitation/emission) using a microplate reader (Synergy HT). Results are expressed as a % of the control. Experiments were performed in quintuplicate.

2.5.2. *Cell morphology*

HBMSCs' morphology was evaluated through fluorescence microscopy, using a Celena S digital imaging system (Logos Biosystems, Villeneuve d'Ascq, France). At determined timepoints, cells were washed and fixed with 3.7% paraformaldehyde. Fixed cells were permeabilized with 0.1% Triton-X and incubated with bovine serum albumin to avoid non-specific interactions. Subsequently, cellular F-actin' cytoskeleton was stained with phalloidin-conjugated Alexa Fluor 488 (Molecular Probes, Eugene, Oregon, USA) and their nuclei were counter-stained with Hoechst 33342 (Enzo Life Sciences, Farmingdale, NY), prior to microscope observation. Assays were performed in triplicate.

2.5.3. *Alkaline Phosphatase activity*

Alkaline Phosphatase (ALP) was quantified in cell lysates that were obtained by adding Triton-X 0.1% to the cultures. Briefly, an alkaline p-nitrophenyl phosphate solution (ALP substrate) was added to cell lysates prior incubation at 37 °C, for 1 h. Then, the reaction was stopped using NaOH 3 M, and the reaction product (p-nitrophenol) was measured at 405 nm using a microplate reader (Synergy HT). Moreover, the levels of total protein (TP) of cell lysates were quantified relying on the Lowry's method, using a DC protein kit (Bio-Rad, Hercules, California, USA), read at 750 nm using the same microplate reader. For each sample, ALP levels were normalized to the corresponding TP levels. Results are expressed as a % of the control. Experiments were performed in quintuplicate.

2.6. Ex vivo assessment using embryonic chick femora model

The influence of morin on the formation of collagenous and mineralized tissues was assessed within the embryonic chick femora organotypic model. Fertilized chick eggs (*Gallus domesticus*) were purchased from a certified seller. Eggs were placed in an automatic egg incubator (Octagon Advance, Brinsea, Weston-super-Mare, UK) until the 11th day of development. Afterwards, femora from euthanized chick embryos were dissected and placed into Netwell® inserts (Costar 3480, 440-µm pore diameter) in 6-well plates. Organotypic cultures were incubated at air/liquid interface at 37°C and 5% CO_2 in air, nourished with α-MEM culture medium supplemented with ascorbic acid (50 µg/mL), penicillin (100 U/mL), streptomycin (100 µg/mL), and amphotericin-B (2.5 µg/mL). After 24 h, femora were cut cross-sectionally in the middle of the diaphysis, and the halves were split. Assembled CP and MCP particles were placed surrounding the diaphyseal area of both halves in experimental groups, while control samples were grown in the absence of any treatment. Culture medium was changed daily, during the subsequent 11 days. Then, femora were fixed in buffered formalin and enclosed in paraffin blocks, prior their sectioning (5 µm-thick). Sections were marked with Alcian Blue with Sirius Red (AB/SR) or Von Kossa (VK) dyes. AB/SR coloration reveals glycosaminoglycans (blue) and collagenous matrix (red), while VK highlights mineralized tissues, producing dark areas. Images were taken using a Zeiss Axiocam 5 Color Camera attached to a Zeiss Axiolab 5 microscope. After photodocumentation, the following histomorphometric indexes were determined using open-source software ImageJ (version 1.54h): Collagen deposition area and mineralized area. Otsu algorithm was used for image segmentation prior measurements [31]. Results are expressed as a % of the control. Assays were performed in triplicate. It is noteworthy that the use of avian embryos within the first two-thirds of development for research purposes is not covered by European (Directive 2010/63/EU) or National (Decreto-Lei n.º 113/2013) legislations, precluding the requirement of regulatory approval for the experimental procedures.

2.7. Statistical analysis

Statistical analysis was accomplished using the SPSS Statistics software (version 28, IBM). The normal distribution (Shapiro-Wilk's test) and homogeneity of variances (Levene's test) were checked. Datasets were assessed for one-way analysis of variance

(ANOVA), followed by Tukey's post hoc test. The significance level was set at $p < 0.05$. Data were displayed as mean ± standard deviation (SD).

3. Results

3.1. Physicochemical characterization and release profile of MCP hydrogels

CP and MCP hydrogels were synthesized via an ionotropic gelation technique, and the prepared gel particles were characterized for morphology, surface charge, chemical composition and morin loading efficiency and release profile.

The interaction between morin and the chitosan-poloxamer hydrogels was investigated by an ATR-FTIR analysis (supplementary image). In brief, since both chitosan and poloxamer possess chemical groups vibrating at similar wavenumbers (cm^{-1}) of morin [32-38], it was challenging to conclusively confirm its presence within the MCP hydrogel. However, it was evident that morin does not chemically bond with either chitosan or poloxamer.

Optical microscopy was applied to observe the morphology and size of CP and MCP particles, while scanning electron microscopy was used for visualizing the surface of morin, CP and MCP particles (Figure 1). Morin (M) presents a rod like shape (Figure 1b) with no other chemical element apart from carbon and oxygen (Figure 1c). The palladium and gold detected in the EDS results (Figure 1c) are from the coating applied to make the sample more conductive. Macroscopically, CP particles (Figure 1d) display a spherical type of morphology, with a subtle and translucent white hue, in addition to an almost uniform and smooth surface (Figure 1e-f). Regarding the MCP particles, a similar morphology can be noted, as well as a yellowish tone and a higher surface roughness (Figure 1g-i). Analysis of zeta potential measurements indicates that both particle types carry a negative surface charge. The average zeta potential value for CP is determined to be −25.5 ± 1.4 mV, while for MCP it is −27.2 ± 1.1 mV, suggesting an overall high stability of the particles [39].

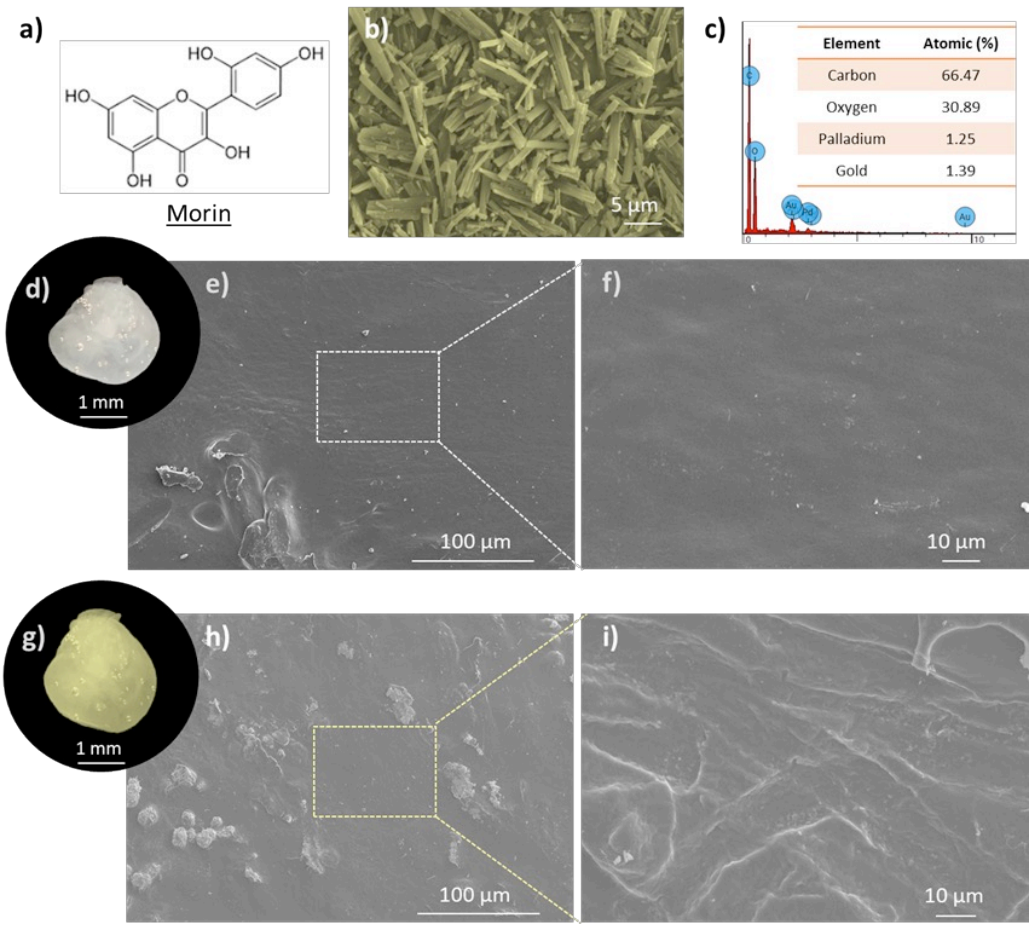

Figure 1. Characterization of morin (M) and the synthesized particles. Morin' chemical structure (a), morphology (b) and chemical composition (c), assessed though SEM and EDS. Light (d, g) and SEM representative images from the surface of CP (e, f), and MCP (h, i) hydrogel particles. (n=3).

UV–vis spectroscopy evaluation revealed an encapsulation efficiency of morin within each MCP particle of approximately 70%, as the total morin quantified in the supernatant per unit reached approx. 35 µg/mL (data not shown). To quantify the amount of morin leached per time from MCP particles, samples were placed into PBS for 24 h and the supernatant was collected at selected timepoints (30 min to 24 h). Throughout the assessed period, morin release peaked at 30 min reaching approximately 50%, and progressively dropped until 6 h (**Figure 2)**. Thus, the percentage of morin release was about 90% after 6 h.

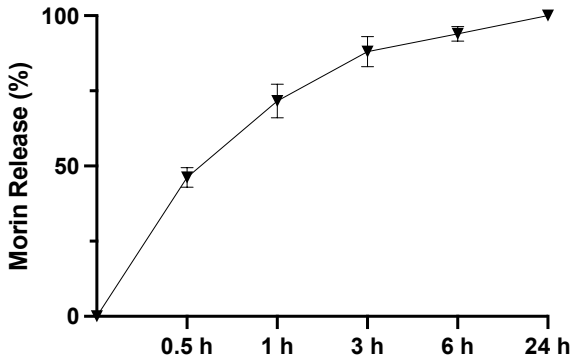

Figure 2. Cumulative released morin from the loaded chitosan-poloxamer (MCP) particles assessed by colorimetric evaluation. (n=3, SD 1.7 – 5.6%).

3.2. Cytotoxicity and pro-osteogenic potential of morin

The cytocompatibility of morin dissolved in DMSO was assessed using *in vitro* HBMSCs cultures. In comparison to control (0 µg/mL of morin), cells incubated for 7 days with morin at 10 and 50 µg/mL presented analogous metabolic activity, evidencing its cytocompatibility (**Figure 3a**). At a concentration as high as 100 µg/mL, metabolic activity was found to be significantly reduced (i.e., approx. 30%) in relation to control and lower concentrations of morin. To evaluate whether morin induced osteogenic effects in early cultures of HBMSCs, ALP activity was quantitatively assessed. As displayed in **Figure 3b**, low concentrations of the compound (i.e. 10 µg/mL) seemed to not induce significant changes in the ALP levels. However, at 50 µg/mL, a significant increase was noted, while a clear reduction was attained with 100 µg/mL. Cell morphology was observed using fluorescence microscopy (**Figure 3**, lower panel). Control cultures were uniform and predominantly forming cellular clusters. HBMSCs exhibited an elongated cytoskeleton, with abundant parallel actin stress fibers across their cytoplasm and spike-shaped membrane protrusions were widespread. Rounded and defined nuclei were evident. Cells from all experimental groups were found to be alike regarding their morphology and organization. Nonetheless, cells incubated with 100 µg/mL morin seemed to be less confluent in comparison to other groups, aligning with the observed reduced metabolic activity.

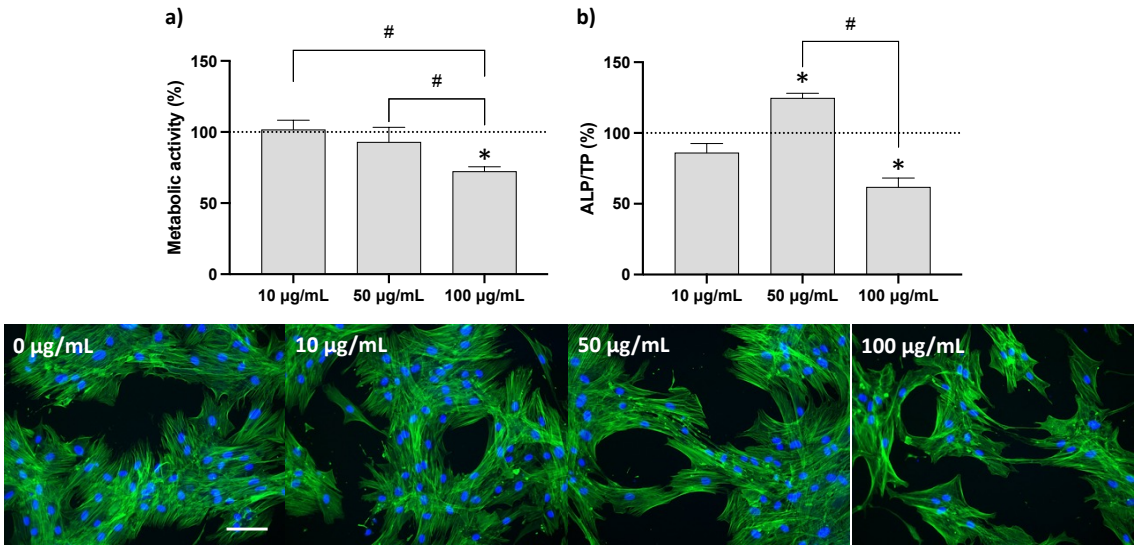

Figure 3. In vitro biological characterization of morin. Normalized metabolic activity (a), quantitative ALP activity (b) and representative fluorescent images of cell morphology (lower panel) of HBMSCs cultivated in osteogenic medium and morin for 7 days. Control (Morin at 0 µg/mL) is set at 100%. Stained F-actin is displayed in green, while nuclei were counter-stained in blue. Scale bar corresponds to 100 µm. * Statistically different from control. # Statistically different from other experimental groups. $p < 0.05$. Metabolic and ALP activities, n=5. Cell morphology, n=3. SD 3.2 to 6.6%.

3.3. Cytotoxicity and pro-osteogenic potential of CP and MCP hydrogels

Firstly, the metabolic activity of HBMSCs was evaluated when cells were incubated with hydrogel leachates. As shown in **Figure 4**, all isolated leachates from CP hydrogel and MCP hydrogel increased the cellular metabolic activity at both timepoints (24 h and 7 days). It is worth noting that the 30-min leachates induced the highest increase at both timepoints, and exposure to MCP hydrogel leachates resulted in significantly higher values in comparison to control, at 24 h (**Figure 4a**), tendency that was kept at 7 days (**Figure 4b**).

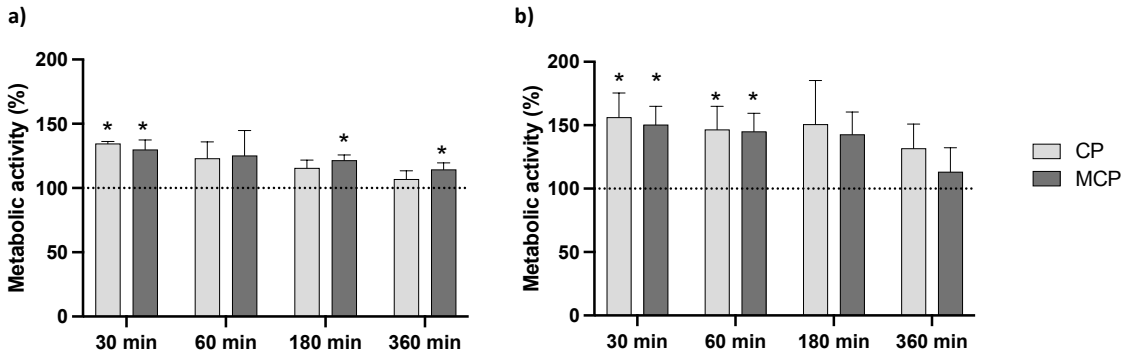

Figure 4. Normalized metabolic activity of HBMSCs cultivated with leachates of chitosan-poloxamer hydrogels (CP and MCP) for 24 h (a) and 7 days (b). X axis values represent the timepoints of leachates' collection. Control (absence of leachates of the referred timepoint) is set as 100%. * Statistically different from control. $p < 0.05$, n=5. SD 5.4 to 19.7%.

HBMSCs were also cultured for 7 days in indirect contact with assembled particles (CP or MCP) using Transwell-mounted plates. As displayed is **Figure 5a**, CP particles promoted an increased metabolic activity compared to the control, while MCP particles values remained similar to the control. Oppositely, only the formulation containing morin induced an upregulation of ALP activity in comparison to control cultures (**Figure 5b**). This is in line with the results observed from morin-only incubation at 50 µg/mL (**Figure 4**). Likewise, HBMSCs' morphology was found to be unaffected in the presence of gels (**Figure 5**, lower panel).

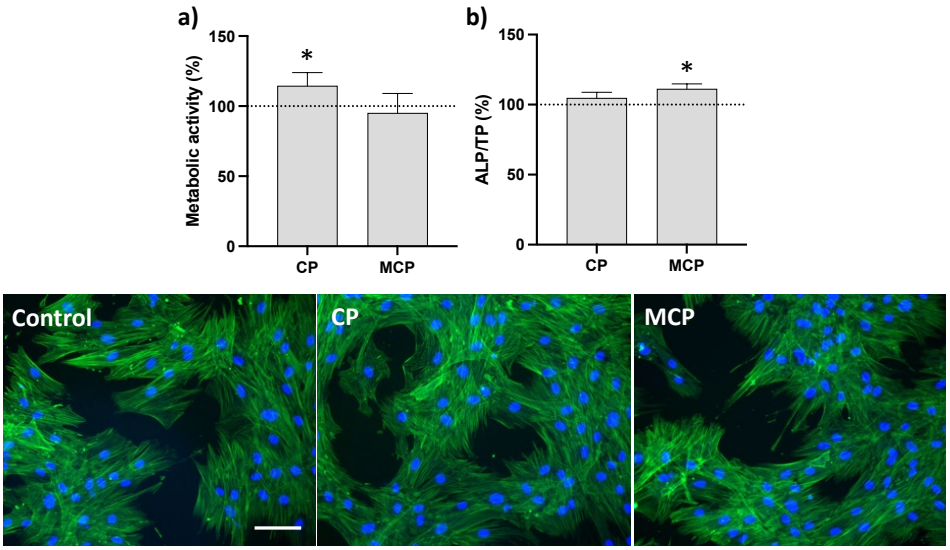

Figure 5. Normalized metabolic and ALP activity (upper panel) and representative fluorescent images (lower panel) of HBMSCs cultivated indirectly with chitosan-poloxamer gels (blank and containing morin) in osteogenic medium for 7 days. Control (C, absence of particles) is set as

100%. F-actin is stained in green, and nuclei were counter-stained in blue. Scale bar is set as 100 µm. * Statistically different from control. $p<0.05$. Metabolic and ALP activities, n=5, Cell morphology, n=3. SD 9.5 – 13.9%.

3.4. Pro-osteogenic effect of CP and MCP particles in organotypic bone model

The pro-osteogenic activity of the particles was further evaluated through their direct contact to organotypic cultures of segmented chicken femora for 11 days. As noted in **figure 6a**, the fractured area from control femora presented an irregular morphology, composed primarily of cartilage (in blue), with diminished amounts of collagen (in red) on the edge of the fracture. Unexpectedly, both particles were stained in red. Moreover, the amount of collagenous tissue on the edge of the fractured femora was greater, particularly in the MCP particle group, confirmed by the quantitative analysis (**Figure 6c**). Differences among groups seemed to be less evident with VK's staining (**Figure 6b**). Nonetheless, experimental groups presented trabeculae through the outer layer of femora, indicating a further developed mineralization, which resulted in significantly increased mineralized area (**Figure 6c**).

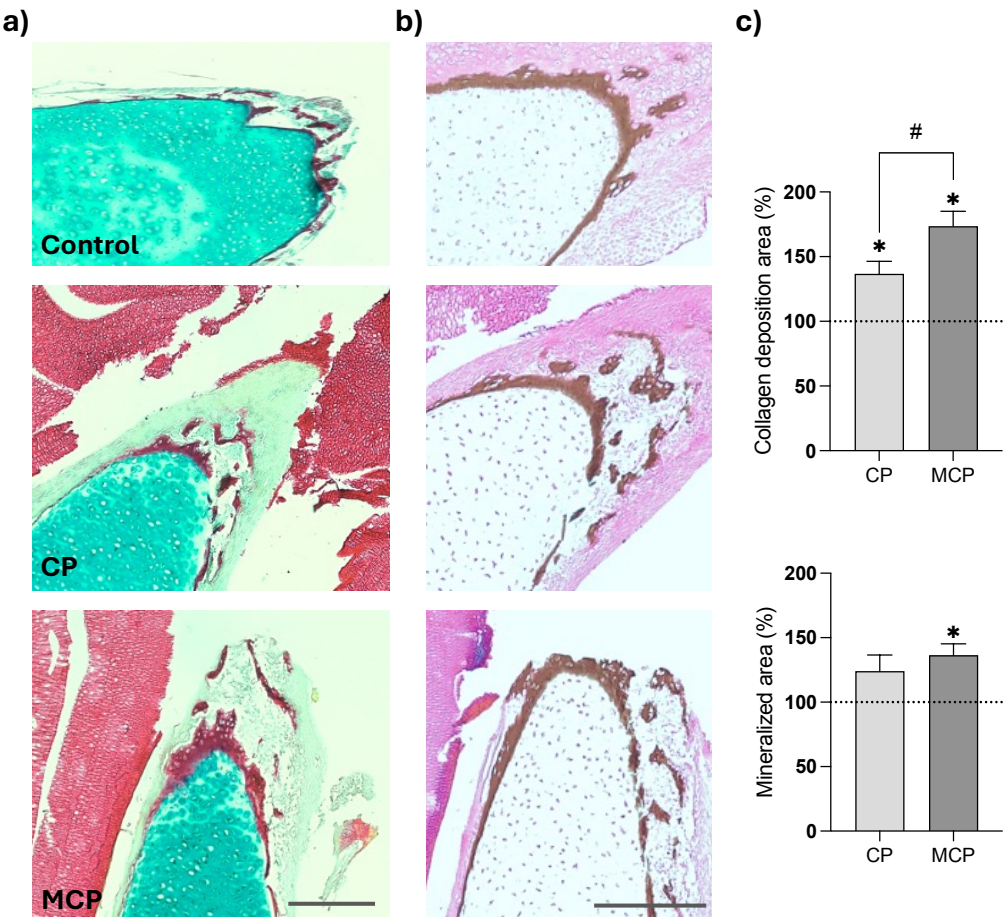

Figure 6. Representative images of histological sections of the organotypic bone model. Femora were fractured and involved with chitosan-poloxamer gels (blank and containing morin). Samples were incubated for 11 days. (a) Femora sections were stained with Alcian Blue with Sirius Red AB/SR (particles were stained in red), and (b) Von Kossa. Scale bar was set as 1 mm. (c) Quantitative analysis of collagen deposition and mineralized area. Control (absence of particles) is set as 100%. *Statistically different from control. # Statistically different from other experimental samples. * $p < 0.05$, n=3. SD 8.8 – 12.4%.

4. Discussion

In this study, chitosan-poloxamer hydrogels loaded with morin hydrate (MCP) were firstly synthesized and physiochemically studied in hydrogels. Based on the ATR-FTIR results of morin and the CP and MCP hydrogels, it was evident that morin does not chemically bond with either chitosan or poloxamer, indicating that morin is entrapped within the matrix without altering its chemical structure, as observed in other studies [40-42]. Analysis of zeta potential measurements indicates that both particle types (CP and MCP) carry a negative surface charge, suggesting an overall good dispersion stability

of the particles. Zeta potential plays a crucial role in evaluating particle dispersion stability and exerts a significant influence on biological response [39]. The magnitude of the zeta potential reflects the repulsive forces within the particle dispersion. It has been observed that hydrogels with a zeta potential value exceeding -25 mV tend to exhibit stability due to electric repulsion among the particles [39].

In the current study, morin alone or loaded in chitosan-poloxamer particles increased the expression of the osteogenic markers: ALP activity, collagen deposition and bone mineralization. Additionally, the cytocompatibility of morin was observed at concentrations of 10 and 50 µg/mL in HBMSCs exposed for 7 days. However, at 100 µg/mL, morin significantly reduced cell metabolic activity. In addition, morin at 50 µg/mL promoted a significant increase on ALP activity by HBMSCs. These findings are in line with previous studies, where morin was found to be cytocompatible at a concentration range of 25–75 µg/mL using mesenchymal stem cells [11] and its half-maximal inhibitory concentration (IC_{50}) was approx. 250 µM (80 µg mL^{-1}) in human leukocytes [16]. Furthermore, *in vivo* investigations demonstrated that morin is well tolerated by humans, with no adverse effects being observed at doses up to 300 mg/Kg [17].

To evaluate the developed formulations with and without morin, two different *in vitro* approaches were performed using HBMSCs. Firstly, the leachates obtained from CP and MCP hydrogels at predetermined timepoints were added to culture media and, secondly, by an indirect incubation, where permeable inserts carrying CP and MCP particles allowed a continuous flux of its leachates to the cultures for 7 days.

Leachates collected after 30 min (the maximum morin release, as observed in Figure 2) induced the highest metabolism increase at 24 h and 7 days timepoints for both hydrogels. On the contrary, when cultured indirectly, CP particles promoted an increased metabolic activity in relation to control, while MCP particles induced a significant increase on ALP activity.

Vimalraj et al. [43] assessed morin and morin-zinc complexes using different cell lines (e.g., human osteoblast-like cells (MG-63), mouse mesenchymal stem cells and rat myoblast cells) and no cytotoxic effects were noted at concentrations up to 60 µM (20 µg/mL). Interestingly, when cultured with morin at this concentration, MG-63 cells exhibited a significant increase in ALP activity, calcium deposition, gene expression of osteogenic-related genes (i.e., RUNX2 and COL1A1) and secretion of osteocalcin (OCN)

and osteonectin, evidencing the osteogenic effects of morin. Similarly, mesenchymal stem cells also showed a remarkable increase on ALP, calcium deposition and the expression of the osteogenic genes Runx2, ALP, OCN and ColA1 when cultured with morin (at 0.6 µg/mL) and osteogenic medium for 14 days [11].

Few studies have examined the osteogenic potential of chitosan-based drug delivery systems containing morin [28, 42]. Ultraviolet-cross-linkable-chitosan carbon dots-morin hydrogel also increased collagen expression and proliferation in chondrocytes, and cartilage and subchondral bone tissue repair in rats [28]. The effectiveness of morin encapsulated chitosan nanoparticles (MCNPs) were evaluated against arsenic induced liver damage in mice. MCNPs suppressed the arsenic induced pro- and anti-apoptotic parameters and attenuated the level of inflammatory mediators [42]. The thermosensitivity of poloxamer 407 is also a key advantage for oral application such as apical periodontitis, since its viscosity tends to increase in temperatures above 30 °C, maintaining the formulation stability for longer periods [27,37]. In addition, studies indicate that poloxamer 407 is also bioactive, fostering wound healing through neo-angiogenesis, cell migration and collagen deposition and maturation [44,45].

Lastly, the osteogenic activity of CP and MCP particles was evaluated on organotypic cultures of chicken femora. This *ex vivo* model preserves the three-dimensional matrix of the bone tissue, fundamental to cellular differentiation and tissue development [46]. Moreover, the developing femur possesses undifferentiated progenitor cells, being highly responsive to external stimuli and may mimic the open apex of teeth, holding translational relevance to the apical development [47].

As observed in Figure 6, experimental groups (CP and MCP particles) presented enhanced collagen deposition in relation to control, and specimens treated with MCP particles showed the highest collagen deposition and mineralized areas on the fractured femora. Comparatively, it has been documented [11] that the administration of morin improved bone regeneration in animal models with calvaria critical defects in a dose-dependent manner (50, 100 and 150 mg/kg/day). In another study, intraperitoneal morin administration in rats with osteoporosis (induced by dexamethasone) increased the number of trabecular bones through the regulation of MAPK signaling pathway [25]. Ultraviolet-cross-linkable-chitosan carbon dots-morin hydrogel also increased collagen

expression and proliferation in chondrocytes, and cartilage and subchondral bone tissue repair in rats [28].

5. Conclusions

This study reports for the first time the suitability of chitosan-poloxamer carriers to be loaded with morin and, further, to be an effective vehicle to delivery polyphenols such as this molecule, presenting a release profile compatible with optimal cellular function.

The chitosan-poloxamer hydrogels were comprehensively evaluated *in vitro*, demonstrating high cytocompatibility. Moreover, the osteogenic potential of morin is demonstrated, as cells exhibit enhanced proliferation and differentiation, evidenced by heightened metabolic and ALP activity, respectively. This is further supported by the results in the *ex vivo* model analysis, where the collagen deposition and mineralization are elicited by the developed particles.

Taken together, the attained data converge to demonstrate the potential of morin loaded chitosan-poloxamer carriers to be used as therapeutic alternative for apical inflammatory condition.

Funding

This work received financial support from FCT/MCTES (UIDB/50006/2020 DOI 10.54499/UIDB/50006/2020) through national funds.

Acknowledgements

The authors acknowledge the support of the i3S Scientific Platform HEMS - Histology and Electron Microscopy Department.

This work received support and help from FCT/MCTES (LA/P/0008/2020 DOI 10.54499/LA/P/0008/2020 and UIDP/50006/2020 DOI 10.54499/UIDP/50006/2020), through national funds.

Data Availability Statement:

The data presented in this study are available on request from the corresponding authors.

Conflicts of Interest:

The authors declare that they have no conflict of interest or financial interests to disclose.

References

[1] Siqueira JF, Magalhães KM, Rôças IN. Bacterial reduction in infected root canals treated with 2.5% NaOCl as an irrigant and calcium hydroxide/camphorated paramonochlorophenol paste as an intracanal dressing. J Endod 2007;33:667–672. http://doi.org/10.1016/j.joen.2007.01.004

[2] Bahuguna R, Jain A, Khan SA, Arvind MS. Role of odanacatib in reducing bone loss due to endodontic disease: An overview. J Int Soc Prev Comm 2016;Dent 6: S175-S181. http://doi.org/10.4103/2231-0762.197183

[3] Krum SA, Chang J, Miranda-Carboni G, Wang CY. Novel functions for NFκB: inhibition of bone formation. Nat Rev Rheumatol 2010; 6:607-611. http://doi.org/10.1038/nrrheum.2010.133

[4] Siqueira Jr JF, Roças IN. Present status and future directions: microbiology of endodontic infections. Int Endod J 2022;55:512–530. http://doi.org/10.1111/iej.13677

[5] Ring KC, Murray PE, Namerow KN, Kuttler S, Garcia-Godoy F. The comparison of the effect of endodontic irrigation on cell adherence to root canal dentin. J Endod 2008;34:1474–1479. http://doi.org/10.1016/j.joen.2008.09.001

[6] Ruksakiet K, Farkas LHN, Hegyi P, Sadaeng W, Czumbel LM, Sang-ngoen T et al. Antimicrobial efficacy of chlorhexidine and sodium hypochlorite in root canal disinfection: a systematic review and meta-analysis of randomized controlled trials. J Endod 2020;46:1032-1041 http://doi.org/10.1016/j.joen.2020.05.002

[7] Diogenes AR, Ruparel NB, Teixeira FB, Hargreaves KM. Translational science in disinfection for regenerative endodontics. J Endod 2014;40:S52-S57. http://doi.org/10.1016/j.joen.2014.01.015

[8] Rafter-M. Apexification: a review Dent Traumatol 2005;21:1-8. http://doi: 10.1111/j.1600-9657.2004.00284.x

[9] Iglesias-Linares A, Yáñez-Vico RM, Sánchez-Borrego E, Moreno-Fernández AM, Solano-Reina E, Mendoza-Mendoza A. Stem cells in current paediatric dentistry practice. Arch Oral Biol 2013;58:227-238. http://doi.org/10.1016/j.archoralbio.2012.11.008

[10] Yang JY, Lee HS. Evaluation of antioxidant and antibacterial activities of morin isolated from mulberry fruits (*Morus alba L*.) J Korean Soc Appl Biol Chem 2012; 55:485–489. http://doi.org/10.1007/s13765-012-2110-9

[11] Wan J, Ma T, Jin Y, Qiu S (2020) The effects of morin on bone regeneration to accelerate healing in bone defects in mice. Int J Immunopathol Pharmacol 34:2058738420962909. http://doi.org/10.1177/2058738420962909

[12] Dias MC, Pinto DCGA, Silva MAS. Plant Flavonoids: Chemical Characteristics and biological activity. Molecules 2021; 26:5377. https://doi.org/10.3390/molecules26175377

[13] Gopal JV. Morin hydrate: botanical origin, pharmacological activity and its applications. Pharmacog J 2013;5:123–126. https://doi.org/10.1016/j.phcgj.2013.04.006

[14] Rajput SA, Wang XQ, Yan HC. Morin hydrate: A comprehensive review on novel natural dietary bioactive compound with versatile biological and pharmacological potential. Biomed Pharmacother 2021; 138:111511. http://doi.org/10.1016/j.biopha.2021.111511.

[15] Caselli A, Cirri P, Santi A, Paoli P. Morin: a promising natural drug Curr Med Chem 2016; 23: 774-791.http://doi.org/10.2174/0929867323666160106150821

[16] Sergediene E, Jönsson K, Szymusiak H, Tyrakowska B, Rietjens IMCM, Čenas N. Prooxidant toxicity of polyphenolic antioxidants to HL-60 cells: Description of quantitative structure-activity relationships FEBS Lett 1999:392–396. http://doi.org/10.1016/s0014-5793(99)01561-6

[17] Cho YM, Onodera H, Ueda M, Imai T, Hirose M A 13-week subchronic toxicity study of dietary administered morin in F344 rats. Food Chem Toxicol 2006;44:891–897. http://doi.org/10.1016/j.fct.2005.12.002

[18] Kopacz M, Woźnicka E, Gruszecka J. Antibacterial activity of morin and its complexes with La (III), Gd (III) and Lu (III) ions. Acta Pol Pharm - Drug Res 2005; 62:65–67.

[19] Huang P, Hu P, Zhou SY, Li Q, Chen WM. Morin inhibits sortase A and subsequent biofilm formation in *Streptococcus mutans* Curr Microbiol 2014; 68:47–52. http://doi.org/10.1007/s00284-013-0439-x

[20] Gutiérrez-Venegas G, Gómez-Mora JA, Meraz-Rodríguez MA, Flores-Sánchez MA, Ortiz-Miranda LF. Effect of flavonoids on antimicrobial activity of microorganisms present in dental plaque. Heliyon 2019; 5(12): e03013. http://doi.org/10.1016/j.heliyon.2019.e03013

[21] Abirami G, Alexpandi R, Durgadevi R, Kannappan A, Veera Ravi A. Inhibitory Effect of morin against *Candida albicans* pathogenicity and virulence factor production: an in vitro and in vivo approaches Front Microbiol 2020;23:11. http://doi.org/10.3389/fmicb.2020.561298

[22] Chemmugil P, Lakshmi PTV, Annamalai A. Exploring morin as an anti-quorum sensing agent (anti-QSA) against resistant strains of *Staphylococcus aureus*. Microb Pathog 2019; 127:304–315. http://doi.org/10.1016/j.micpath.2018.12.007

[23] de Farias AL, Meneguin AB, da Silva Barud H, Brighenti FL. The role of sodium alginate and gellan gum in the design of new drug delivery systems intended for antibiofilm activity of morin. Int J Biol Macromol 2020;162:1944–58. http://doi.org/10.1016/j.ijbiomac.2020.08.078

[24] Farias AL, Arbeláez MIA, Meneguin AB, Barud HDS, Brighenti FL. Mucoadhesive controlled-release formulations containing morin for the control of oral biofilms. Biofouling 2022;38:71-83. http://doi.org/10.1080/08927014.2021.2015580.

[25] Wang C, Wan X, Li Y, Zhang H, Zhang L. Morin protects glucocorticoid-induced osteoporosis through regulating the mitogen-activated protein kinase signaling pathway. J Nat Med 2018;72:929-936. http://doi.org/10.1007/s11418-018-1228-4.

[26] Mu M, Li X, Tong A, Guo G. Multi-functional chitosan-based smart hydrogels mediated biomedical application. Expert Opin Drug Deliv 2019; 16:239-250. http://doi.org/10.1080/17425247.2019.1580691.

[27] Dumortier G, Grossiord JL, Agnely F, Chaumeil JC. A review of poloxamer 407 pharmaceutical and pharmacological characteristics Pharm Res 2006;23:2709-2728. http://doi.org/10.1007/s11095-006-9104-4

[28] Qu Y, Guan Z, Nan F, Liu S, Liu L. Effect and mechanism of ultraviolet-cross-linkable chitosan-carbon dots-morin hydrogel treating for rat cartilage injury. Zhongguo Xiu Fu Chong Jian Wai Ke Za Zhi. 2022;36:1524-1533. http://doi.org/10.7507/1002-1892.202208121.

[29] Huang C, Peng L, Xu X, Lu Y, Wang X, Lan Z et al. Preparation and characteristics of a thermosensitive *in situ* gel loaded with chitosan nanoparticles for optimal ocular delivery of chloramphenicol. J Drug Deliv Sci Tech 2023;89:104962. https://doi.org/10.1016/j.jddst.2023.104962

[30] Dardouri M, Bettencourt A, Martin V, Carvalho FA, Santos C, Monge N et al. Using plasma-mediated covalent functionalization of rhamnolipids on polydimethylsiloxane towards the antimicrobial improvement of catheter surfaces. Biomater Adv 2022;134:112563. http://doi.org/10.1016/j.msec.2021.112563.

[31] IEEE Transactions on Systems, Man, and Cybernetics. Volume: 9, Issue: 1, January 1979. Available on the website: https://ieeexplore.ieee.org/document/4310076 .

[32] Cunha C, Marinheiro D, Ferreira BJML, Oliveira H, Daniel-da-Silva AL. Morin hydrate encapsulation and release from mesoporous silica nanoparticles for melanoma therapy. Molecules. 2023;28:4776. http://doi.org/10.3390/molecules28124776.

[33] Singh P, Ansari Z,Ray S, Bandyopadhyay B, Sen K. Effect of γ-irradiation on ruthenium-morin nanocomposite for trace detection of Ce(IV), Ce(III) and Dy(III). Mat Chem Phys 2020;248:122949. http://doi.org/ 10.1016/j.matchemphys.2020.122949.

[34] Dimitrić Marković JM, Marković ZS, Krstić JB, Milenković D, Lučić B, AmićD. Interpretation of the IR and Raman spectra of morin by density functional theory and comparative analysis. Vibrat Spectr 2013;64:1-9. doi:https://doi.org/10.1016/j.vibspec.2012.10.006.

[35] Drabczyk A, Kudłacik-Kramarczyk S, Głąb M, Kędzierska M, Jaromin A, Mierzwiński D, Tyliszczak B. Physicochemical investigations of chitosan-based hydrogels containing *Aloe Vera* designed for biomedical use. Materials (Basel) 2020;13:3073. http://doi.org/10.3390/ma13143073.

[36] Leyva-Gómez G, Santillan-Reyes E, Lima E, Madrid-Martínez A, Krötzsch E, Quintanar-Guerrero D et al. A novel hydrogel of poloxamer 407 and chitosan obtained by gamma irradiation exhibits physicochemical properties for wound management. Mater Sci Eng C Mater Biol Appl. 2017;.74:36-46. http://doi.org/10.1016/j.msec.2016.12.127.

[37] Vyas V, Sancheeti P, Karekar P, Shah M, Pore Y (2009) Physicochemal characterization of solid dispersion systems of tadalafil with poloxamer 407. Acta Pharm 59:453-461. https://doi.org/10.2478/v10007-009-0037-4.

[38] Garala K, Joshi P, Shah M, Ramkishan A, Patel J. Formulation and evaluation of periodontal in situ gel. Int J Pharm Investig. 2013;3:29-41. https://doi.org/10.4103/2230-973X.108961

[39] Aibani N, Rai R, Patel P, Cuddihy G, Wasan EK. Chitosan Nanoparticles at the Biological Interface: Implications for Drug Delivery. Pharmaceutics 2021;13:1686. http://doi.org/ 10.3390/pharmaceutics13101686.

[40] Yazdanshenas R, Gharib F. Spectrophotometric determination of preferential solvation and solvation shell composition of morin hydrate in some water-aliphatic alcohol mixed solvents. J Mol Liq 2017;243:414-419. https://doi.org/10.1016/j.molliq.2017.08.064.

[41] Cruz MAE, Tovani CB, Favarin BZ, Soares MPR, Fukada SY, Ciancaglini P, Ramos AP. Synthesis of Sr-morin complex and its in vitro response: decrease in osteoclast differentiation while sustaining osteoblast mineralization ability. J Mater Chem B 2019;7:823-829. http://doi.org/10.1039/c8tb02045k

[42] Mondal S, Das S, Mahapatra PK, Saha KD. Morin encapsulated chitosan nanoparticles (MCNPs) ameliorate arsenic induced liver damage through improvement of the antioxidant system and prevention of apoptosis and inflammation in mice. Nanoscale Adv 2022;13:2857-2872. http://doi.org/10.1039/d2na00167e.

[43] Vimalraj S, Subramaniyam R, Saravan S, Deepak T, Murugan K, Dhanasekaran A. Zinc chelated morin promotes osteblast differentiation over its uncomplexed counterpart. Proc Biochem 2019;82: 167-172. http://doi.org/10.1016/j.procbio.2019.04.008

[44] Chen Y, Lee JH, Meng M, Cui N, Dai CY, Jia Q et al. An Overview on Thermosensitive Oral Gel Based on Poloxamer 407. Materials (Basel) 2021;14:4522. http://doi.org/10.3390/ma14164522.

[45] Kant V, Gopal A, Kumar D, Gopalkrishnan A, Pathak NN, Kurade NP et al. Topical pluronic F-127 gel application enhances cutaneous wound healing in rats. Acta Histochem 2014;116:5-13. http://doi.org/10.1016/j.acthis.2013.04.010.

[46] Garbieri TF, Martin V, Santos CF, Gomes PS, Fernandes MH. The Embryonic Chick Femur Organotypic Model as a Tool to Analyze the Angiotensin II Axis on Bone Tissue. Pharmaceuticals (Basel) 2021;14:469. http://doi.org/10.3390/ph14050469.

[47] Araújo R, Martin V, Ferreira R, Fernandes MH, Gomes OS. A new ex vivo model of the bone tissue response to the hyperglycemic environment - The embryonic chicken femur organotypic culture in high glucose conditions. Bone 2022;158:116355. http://doi.org/10.1016/j.bone.2022.116355.

List of Figure legends:

Figure 1. Characterization of morin (M) and the synthesized particles. Morin' chemical structure (a), morphology (b) and chemical composition (c), assessed though SEM and EDS. Light (d, g) and SEM representative images from the surface of CP (e, f), and MCP (h, i) hydrogel particles. (n=3).

Figure 2. Cumulative released morin from the loaded chitosan-poloxamer (MCP) particles assessed by colorimetric evaluation. (n=3, SD 1.7 – 5.6%).

Figure 3. In vitro biological characterization of morin. Normalized metabolic activity (a), quantitative ALP activity (b) and representative fluorescent images of cell morphology (lower panel) of HBMSCs cultivated in osteogenic medium and morin for 7 days. Control (Morin at 0 µg/mL) is set at 100%. Stained F-actin is displayed in green, while nuclei were counter-stained in blue. Scale bar corresponds to 100 µm. * Statistically different from control. # Statistically different from other experimental groups. $p < 0.05$. Metabolic and ALP activities, n=5. Cell morphology, n=3. SD 3.2 to 6.6%.

Figure 4. Normalized metabolic activity of HBMSCs cultivated with leachates of chitosan-poloxamer hydrogels (CP and MCP) for 24 h (a) and 7 days (b). X axis values represent the timepoints of leachates' collection. Control (absence of leachates of the referred timepoint) is set as 100%. * Statistically different from control. $p < 0.05$, n=5. SD 5.4 to 19.7%.

Figure 5. Normalized metabolic and ALP activity (upper panel) and representative fluorescent images (lower panel) of HBMSCs cultivated indirectly with chitosan-poloxamer gels (blank and containing morin) in osteogenic medium for 7 days. Control (C, absence of particles) is set as 100%. F-actin is stained in green, and nuclei were counter-stained in blue. Scale bar is set as 100 µm. * Statistically different from control. $p<0.05$. Metabolic and ALP activities, n=5, Cell morphology, n=3. SD 9.5 – 13.9%.

Figure 6. Representative images of histological sections of the organotypic bone model. Femora were fractured and involved with chitosan-poloxamer gels (blank and containing morin). Samples were incubated for 11 days. (a) Femora sections were stained with Alcian Blue with Sirius Red AB/SR (particles were stained in red), and (b) Von Kossa. Scale bar was set as 1 mm. (c) Quantitative analysis of collagen deposition and mineralized area. Control (absence of particles) is set as 100%. *Statistically different from control. # Statistically different from other experimental samples. * $p < 0.05$, n=3. SD 8.8 – 12.4%.